Post-buckling Strength of Welded Steel I-Girders with Corrugated Webs

Xuqun Lin, Harry Far*

School of Civil and Environmental Engineering, Faculty of Engineering and Information Technology, University of Technology Sydney (UTS), Australia

Abstract

Steel I-section-plate girders with corrugated webs have been used worldwide as they provide more stability and light beam features in practical design. It is known from previous investigations that due to having numerous favourable properties, the corrugated-web beams have been used in different areas of structural engineering. Considering the raising popularity of using CWBs in steel design, some practical aspects of CWBs need to be investigated further, in which post-buckling strength is one of the most critical strengths that should be precisely estimated. To fulfill this requirement regarding the post-bucking strength determination for structural designers community, a numerical investigation has been conducted in this study to determine the moment capacity reduction factors for steel I girders with corrugated-web profile and to compare reduction factor values extracted from EN1993-1-5 (2006), AS4100 (1998), and finite element analysis. Theory of Ultimate Limit State design has been adopted in accordance with AS4100 (1998) along with considering geometric and material non-linearity in the numerical analyses in SAP2000 software. Eventually, the results of the parametric study have been compared and discussed leading to presenting practical recommendations on the design of CWBs for bending strength.

Keywords: *Post-buckling Strength; Corrugated Web Beams; Optimisation; SAP2000; Ultimate Limit State Design*

1. Introduction and Background

Steel I-section-plate girders with corrugated webs have been used worldwide as major constructional elements in different structural designs. The major advantage of corrugated web beams (CWBs) is that the corrugated profile has enhanced the ability to resist buckling in the weak out-of-plane direction, which may reduce the application of web stiffeners (Divaha & Joanna 2018). This fact has made CWBs a popular research topic in the recent decades. Many researchers (e.g. Yazzed 2007; Abbas et al. 2006; Elchalakani et al. 2018) have stated that the nature of corrugation in the webs has been found to increase the bending and shear stiffness values, in which the stability of the beams is strengthened and the thickness of the webs can be thinner to resist the same level of loads compared to traditional flat-web beams. Due to having better stability than conventional flat-web beams, CWBs are being utilised in many countries with raising popularity (Huang et al. 2004: Dubina et al. 2015; Divaha & Joanna 2018). As a reasonable alternative for flat-web beams, CWBs have gained numerous applications in practice as load-resistant components for large-building beams and for runway segments of bridge designs (Li et al. 2019).

According to available literatures, different aspects of CWBs have been investigated. Abbas et al. (2006) performed several experiments regarding the shear strength of CWBs. In their tests, web imperfections, which maybe caused due to manufacturing process or nonlinearity of materials, were considered to eliminate the potential errors, and the authors suggested that the corrugated profile of the webs provided enhanced stability in shear resistance. Baraket et al. (2018) analysed the shear behaviour of CWBs against different buckling modes, where they have found that the shear stiffness of CWBs will be increased 1.5 to 2 folds compared to the strength of traditional flat-web beams. According to Aggarwal et al. (2018), the strength of the corrugated-web girders was not compromised with a possible 30% of reduction in cost of materials after several tests of shear buckling of corrugated-web girders. Similarly, Divaha & Joanna (2018) concluded that a cost savings up to 30% could be achieved by using thinner webs in this type of beams. In their experimental investigations of twelve different sets, they summarised that beams with corrugation nature in webs had lesser deformations and higher flexural stiffness in comparison to ordinary beams. According to Lin et at. (2018), 20% of the material weight and one fifth of the depth of beams section can be saved to achieve the optimised design while maintaining the same level of capacity compared with the corresponding parent welded beams. They also suggested that the noticeable cost saving can be achieved by replacing the selected welded beam with a CWB with equal capacity and lower section depth in the design of multiple-storey buildings, where the saved height in beams can be used to add additional floors to the proposed building design, which can be recognised as a more economical design. Several researchers (Maali 2019; He et al. 2017; Zhou et al. 2019) found that the utilisation of corrugations in the web has improved the beam performances in flexural resistance and the efficiency of materials. All the above-mentioned information of corrugated-web beams proved the fact that CWBs can be used in practical designs with lesser cost of materials, lower values of displacements, and better stability against buckling.

* Corresponding author: Senior Lecturer in Structural Engineering, School of Civil and Environmental Engineering, Faculty of Engineering and Information Technology, University of Technology Sydney (UTS), Building 11, Level 11, Broadway, Ultimo NSW 2007 (PO Box 123), Email: harry.far@uts.edu.au

It is known from the previous researches that CWBs are commonly used in different areas of structural designs, where some practical aspects of CWBs should be highly analysed. According to Walsh et al. (2018), beams are the essential elements to support each floor and the loads will be transmitted to the foundation by columns. Hence, the strengths of structural members after loadings should be clearly and precisely estimated to avoid potential risks of structural failures. Post-buckling strength is one of the most significant design aspects for structural members, which represents the actual strength of beams subjected to loadings. The most commonly used approach is to apply a reduction factor, in which researchers may consider different types of restrictions to achieve a more reasonable results for structural designs. Yazeed (2007) set up four girders with corrugation to investigate the post-buckling strengths. The author utilised a reduction factor of C_b to calculate the real moment resistance values as follows:

$$C_b = \frac{12.5 * M_{max}}{3M_1 + 4M_2 + 3M_3 + 2.5M_{max}} \tag{1}$$

where M_1, M_2, M_3 are the absolute moment results located at quarter point, mid-span point, and three-quarter point of the analysed beams, and M_{max} is the maximum bending moment resisted by the CWBs. However, after comparison with experimental results, this proposed formula was proved to underestimate the bending capacity of the beams, but it is deemed a conservative approach for design purposes.

Elchalakani et al. (2018) performed parametric studies on the moment resistance of different girders with corrugation profile. They recommended that many aspects, such as residual stresses and imperfections, should be considered to get accurate results, which were improved by using the finer mesh in the finite element analysis. As a result, the reduction of 1 to 3% on the moment capacity could be achieved. By using Equation (2), Elchalakani et al. (2018) estimated relatively acceptable values to describe the flexural behaviour of corrugated-web beams. However, the theoretical results of this approach would be affected by multiplying an imperfection factor α_L, which would amplify the final values from theoretical calculations with a ratio of 1.01 to 1.15, which can be recognised that this equation may overestimate the bending capacity.

$$M_{cr} = \frac{\pi}{L}\sqrt{EI_y GJ(1 + \frac{\pi^2}{L^2}\frac{EC_w}{GJ})} \tag{2}$$

where E is the Young's modulus, I_y is the second moment of inertia in the mirror axis, L is the corrugation length, G is the shear modulus, J is the torsion constant. Cw is the imperfection factor.

Several researchers (Abbas et al. 2003; Alandkar & Limaye 2013; Ashrawi et al. 2016) have undertaken some comprehensively parametric studies to estimate post-buckling bending resistance. However, many of those researchers unexpectedly overestimated or underestimated the post-buckling strengths of CWBs in their numerical studies with linear analysis. In their parametric settings, they paid little attention to corrugation sizes and imperfections of the webs while these two factors were necessary to be considered to get accurate results. Nevertheless, all the above-mentioned researchers performed investigative research works to calculate the post-buckling strengths of CWBs, some of those functional works adopted linear-analysis approach or made inappropriate assumptions for investigating the bending nature of CWBs under different types of loads.

As a reasonable alternative to ordinary beams, CWBs have been utilised in some regions of Australia without appropriate methodology to estimate the post-buckling strength. Moreover, AS 4100(1998), the steel structures standard in Australia, demonstrates all essential structural requirements in the steel design field but it does not contain reduction factors for CWBs post-buckling strength calculations. Therefore, an acceptable method for calculating the post-buckling strength of unrestrained corrugated-web beams is highly required to enable Australian engineering community design this type of beams accurately.

2. Theoretical Background

Aiming to find an acceptably appropriate reduction factor in bending moment calculations of CWBs for Australian steel designers, EN 1993-1-5 (2006) and AS4100 (1998) are used in this study to carry out a comprehensive numerical and parametric investigation. EN1993-1-5 (2006), the standard of steel structures – plated structural elements in European Union, includes the following relationships to calculate the moment reduction factor f_T by considering the shear action on the bending computation:

$$f_T = 1 - 0.4 * \sqrt{\frac{\sigma_{x,M_z}}{\frac{f_{yf}}{\gamma_{MO}}}} \tag{3}$$

where σ_{x,M_z} is the maximum value of additional stress resulted from transverse bending moment from Equation (4), f_{yf} is yield strength of the beam flange, γ_{MO} is the partial factor for stress check.

$$\sigma_{x,M_z} = \frac{M_{z,max}}{I_f} * \frac{b_f}{2} \tag{4}$$

where $M_{z,max}$ is the maximum transverse bending moment from Equation (5),

$$M_{z,max} = \frac{V * a_3}{2 * d_w} * (2 * a_1 + a_4) \tag{5}$$

Where a_1 is equal to a quarter of the corrugation length L, a_4 is equal to half of the corrugation length L, a_3 is equal to 2 times the amplitude of the corrugation as shown in Figure 1.

These highly structured set of relationships were validated by Kovesdi et al. (2012) & Dunai et al (2016). After comprehensive numerical analysis and computer-based simulation, both studies have concluded that this reduction factor, which is resulted from the interaction equations, is accurate enough to be used in the design of CWBs. Hence, the above-mentioned proposed conservative design equations will be used to generate theoretical results of the post-buckling strengths, which will be used to be compared with the results generated from FE simulations via using the material properties and other limitations stated in Australian Standards.

Section 5 of AS4100 (1998) includes the numerical approach to calculate the post-buckling strength for flat-web steel beams, in which the reduction factor is a combination of α_m and α_s. This study will utilise this method to estimate the real strength of corrugated-web beams after being under different load conditions. The modification factor α_m shall be determined from Table 5.6.1 of AS4100 or Equation (6) below:

$$\alpha_m = \frac{1.7 M_{max}}{\sqrt{(M_2)^2 + (M_3)^2 + (M_4)^2}} \leq 2.5 \tag{6}$$

where $M_2, M_3,\ M_4$ are the absolute moment results located at quarter point, mid-span point, and three-quarter point respectively of the CWB, and the M_{max} is the maximum design bending resistance.

The slenderness factor α_s is calculated from Equations (7) and (8) as follows:

$$\alpha_s = 0.6 * [\sqrt{\left(\frac{M_s}{M_o}\right)^2 + 3} - \frac{M_s}{M_o}] \tag{7}$$

$$M_o = \sqrt{\left(\frac{\pi^2 E I_y}{l_e^2}\right) [\ GJ + \left(\frac{\pi^2 E I_w}{l_e^2}\right)]} \tag{8}$$

where E is the Young's modulus, I_y is the second moment of inertia in the mirror axis, I_e is the effective beam length, G is the shear modulus, J is the torsion constant, I_w is the warping constant.

α_m is a modification factor which depends on the shape of the bending moment diagram. Consequently, the shape of the beam web does not influence this factor. As a result, flat-web and corrugated-web steel sections can use the same α_m values. Therefore, this study will focus on determining the slenderness factor α_s for corrugated-web steel sections and utilises the α_m values prescribed in AS4100 (1998). All the necessary material information of CWBs will be selected from the cross-sectional geometry and properties of the welded beams listed in the Hot Rolled and Structural Steel Products property Tables (2020). Moreover, AS/NZS 1170.1 (2002) will be used to calculate the design actions and perform any required safety checks, including the type of loads combination, modification factors of design loads, and buckling load factors check.

3. Methodology

A sample elevation of CWB numerical model is illustrated in Figure 1 to show the geometry details of the numerical simulation in this study. Figure 1 clearly illustrates one of the CWB model for this study, where the fundamental dimensions of the cross-sectional geometry will be the same as the values listed in the Hot Rolled and Structural Steel Products property tables (2020). The webs of the beams then were replaced by the corrugation profile, in which the corrugation angle was 30° and the corrugation length was 400mm as suggested by Lin et al. (2018).

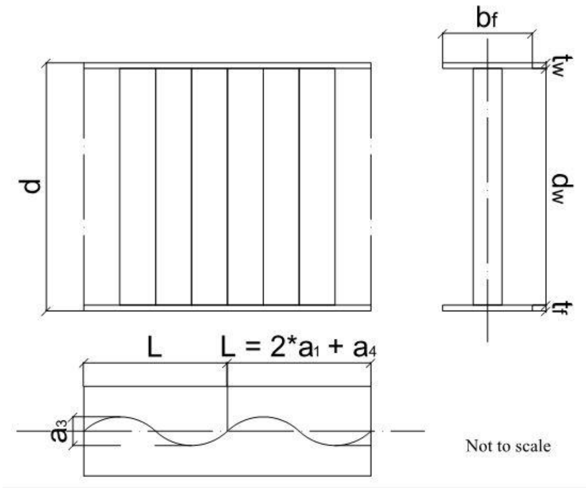

Figure 1. Sample elevation of a CWB

A comprehensive parametric investigation has been carried out, using SAP2000 non-linear finite element analysis software (Computers and Structures 2020), to investigate the maximum bending moments of CWBs under two different conditions, which will be used to generate the reduction factors to compare with reduction factors from the theoretical calculations. One group of CWBs are fully restrained at the compression flange, being top flange, and hence the lateral torsional buckling is prevented. The other group of CWBs with the same dimensions and material properties are unstrained at the top flanges, which could only resist smaller portion of the bending moments compared to ones from fully restrained group. The elastic buckling analysis will be carried out before estimating the moment ratio, being the required values of the reduction factor, where all buckling load factors were greater than 1 based on each CWB's design action combination for bending strength in accordance with AS/NZS 1170.1 (2002). Based on the tested results coming from the two groups, the ratio between the CWBs with fully restrained and unrestrained CWBs can be calculated. Finally, the theoretical results of using EN1993-1-5 (2006) method will be compared with simulation-based results to see the accuracy of the models, and then conservative equations for Australian steel designers to calculate the post-buckling strength of CWBs for unrestrained beams will be developed.

3.1 Numerical Simulation Assumptions

The following aspects were considered to perform appropriate numerical simulation using SAP2000 finite element software. A typical demonstration of meshed model is given in Figure 2.

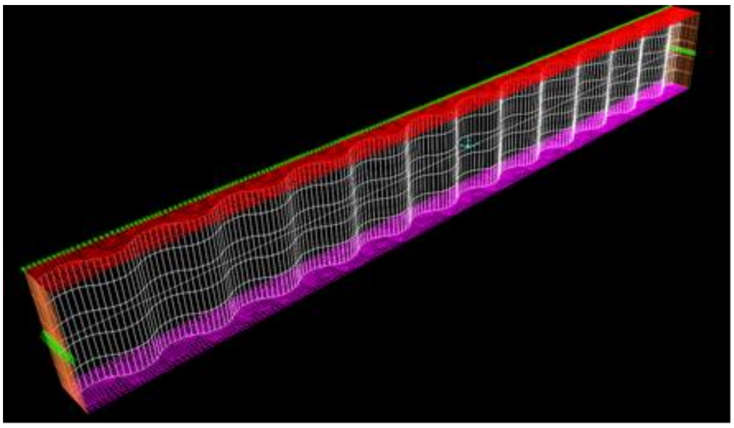

Figure 2. Illustration of a 3-D beam model with end stiffeners

- The examined length of CWBs is selected as 5 metres, since it is in the middle range of 3-7 metres, which is typically utilised in Australian buliding industry .
- To ensure a safe design, the stress levels of all models should be below 0.9fy.
- The components of CWBs were modelled using the FE simulation standard shell elements contained in SAP2000. Details of a representative FE model are shown in Figures 2 and 3.
- The supporting condions of CWBs were simply supported, where the critical top flange was fully restrained against lateral buckling for one group and the other group was unrestrained.

- As depicted in Figure 3, two stiffner plates were placed at both ends of each CWB, which provied a twisting constraint at both ends of the beam. Pin and roller supports were modelled by constraining the nodes at the stiffener's mid-depth. The same stiffener nodes were also constrained at only one end in the beam's longitudinal direction to eliminate the effects of rigid body displacement.
- This study will analyse the design flexural stress of CWBs, where all stages will be limited to elastic stage, since the load inceasement is stopped when the stresses on each CWB are approaching the stress limits.

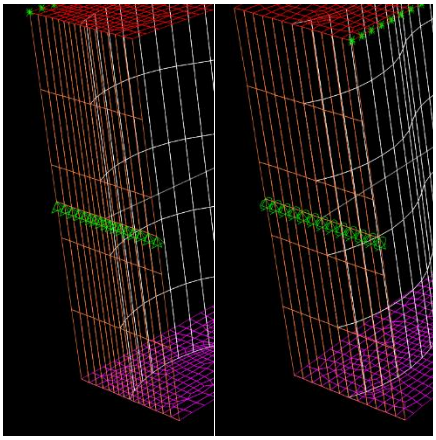

Figure 3. Details of pin supports and roller supports at beam ends

3.2 Design and Analysis Parameters

The maximum load that each CWB can safely resist in terms of uniformly distributed load *w*, was calculated as the distributed load required for the corresponding parent ordinary beam to reach its ultimate limit resistance for bending about the major principal axis. Adopting the Ultimate Limit State (ULS) design theory according to AS4100 (1998), the ultimate moment capacity is reached when the normal stress σ in the extreme fibre reaches the value of σ = Φf_y, where the capacity reduction factor Φ is equal to 0.9 and f_y is the yield stress.

The extreme fibre stress is equal to

$$\sigma = \frac{My}{I} \tag{9}$$

where, I is the second moment of inertia and y is the distance from the centroid axis to the top fibre of the beam. The mid-span moment M of a simply supported beam of length L is given by

$$M = \frac{\omega * L^2}{8} \tag{10}$$

From equations (9) and (10), the load w can be extracted as follows:

$$\omega^* = \frac{14.4 f_y * I}{d * L^2} \tag{11}$$

The value of ω^*established in equation (11) is assumed to represent the design load combination for flexural strength in accordance with AS/NZS 1170.1 (2002) in the form of ω^* = (1.2DL+1.5LL), with DL and LL representing respectively Dead Load and Live Load. Assuming DL =3LL leads consequentially to DL= ω^*/ 1.7 and LL = ω^* / 5.1 and thereby enable the analysis of an additional load case to ensure satisfying the deflection limit states for the design load case of AS/NZS 1170.1 given by ω^{Δ} =(DL+0.7LL), which equates to ω^{Δ}=0.725 ω^*.

Using these starting values to investigate the models in two groups, a trial and error process was followed in this research in order to find the maximum bending moment of each CWB. The trial and error process was stopped when the stress levels approached 0.9* f_y for the bending stress or 0.6* f_y for the shear stress. In this study, two different kinds of structural steel grades have been used, consisting of 300PLUS-300 and 300PLUS-280, while the mass density of structural steel is equal to 7849 kg/m^3. Other necessary material properties are dtabulated in Table 1.

Table 1. Illustrations of Material types of WB beams.

	Grade	f_y *(MPa)*	f_u *(MPa)*	*E (MPa)*	*G (MPa)*
700WB115	*300PLUS-300*	300	*440*	*200000*	*82*
700WB130	*300PLUS-280*	300	*440*	200000	82
700WB150	*300PLUS-280*	280	*440*	200000	82

800WB122	*300PLUS-300*	300	*440*	200000	82
800WB146	*300PLUS-300*	300	*440*	200000	82
800WB168	*300PLUS-280*	280	*440*	200000	82
900WB175	*300PLUS-300*	300	*440*	200000	82
900WB218	*300PLUS-280*	280	*440*	200000	82
900WB257	*300PLUS-280*	280	*440*	200000	82
1000WB215	*300PLUS-300*	300	*440*	200000	82
1000WB258	*300PLUS-280*	280	*440*	200000	82
1000WB296	*300PLUS-280*	280	*440*	200000	82
1200WB249	*300PLUS-280*	280	*440*	200000	82
1200WB278	*300PLUS-280*	280	*440*	200000	82
1200WB313	*300PLUS-280*	280	*440*	200000	82

4. Validation of the Developed Numerical Model

Several studies (e.g. Martins et al. 2012; Calenzani et al. 2012; Oliveira et al. 2016) have carried out on structural behaviours of corrugated-web beams. The numerical results obtained from this study have been compared against the results of experiments performed by Martins et al. (2012) to verify the accuracy of the numerical simulation model used in this study. Martins et al. (2012) performed functional tests on three full-scale composite connections for CWBs, including PSS 600×150×12.5×2.0 for specimens 1 and 2 and PSS 600×150×8/ 12.5×2.0 for specimen 3. Considering the similar beam shape and size to the developed model in this study, the specimen 1 has been selected for numerical and parametric validation, where the same FE technique with shell elements used in this study was applied to the tested beam to generate necessary results for comparison. The FE results obtained using the same technique adopted to corrugated-web beam models in this study have been validated against the load-displacement curve published by Martins et al. (2012) in Figure 4.

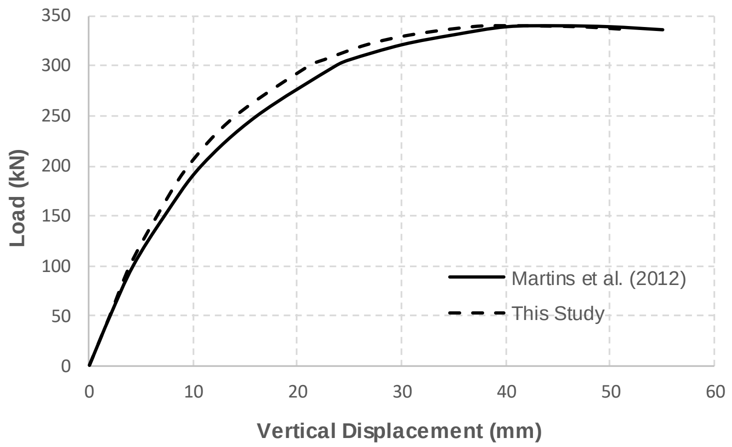

Figure 4. Load-deflection curves estimated by the numerical model developed in this study with the experimental data reported by Martins et al. (2012).

Figure 4 apparently illustrates that the trends and the results of the numerical analysis, obtained from the developed SAP2000 simulation model in this study, show good agreement and consistency with the experimental results reported by Martins et al. (2012). As a result, the developed numerical model in this study can reasonably and acceptably represent the real physical and mechanical behaviours of steel beams with corrugated webs. The validity of the developed SAP2000 numerical models has been verified by the good agreement between the experimental results and the numerical predictions in this study. Hence, predictions give high degrees of confidence in the practical use of the developed numerical model.

5. Numerical and Analytical Investigation

5.1 Finite Element Analysis

Using SAP2000 finite element software, 3 different welded beams in 5 beam grades were selected to carry out the investigation, in which the flat webs will be replaced by a corrugation profile, namely 700CWB115, 800CWB122, 900CWB175, 1000CWB215, and 1200CWB249 respectively. Starting with the basic uniformly distributed load ω^*

(UDL), the maximum UDL can be found by trial and error method in which the stress levels approached 0.9* f_y for the bending stress or 0.6* f_y for the shear stress. The summery of the important analysis results is given in Table 2.

Table 2. Summary of forces of CWBs with fully restraint

	M(kNm)*	*ω*(kN/m)*	*M_1(kNm)*	*M_2(kNm)*	*M_3(kNm)*	*V(kN)*
700CWB115	1000	320	750	1000	750	800
700CWB130	1250	400	937.5	1250	937.5	1000
700CWB150	1400	448	1050	1400	1050	1120
800CWB122	1200	384	900	1200	900	960
800CWB146	1550	496	1162.5	1550	1162.5	1240
800CWB168	1740	556.8	1305	1740	1305	1392
900CWB175	1980	633.6	1485	1980	1485	1584
900CWB218	2450	784	1837.5	2450	1837.5	1960
900CWB257	3000	960	2250	3000	2250	2400
1000CWB215	2500	800	1875	2500	1875	2000
1000CWB258	3000	960	2250	3000	2250	2400
1000CWB296	3520	1126.4	2640	3520	2640	2816
1200CWB 249	3000	960	2250	3000	2250	2400
1200CWB278	3500	1120	2625	3500	2625	2800
1200CWB313	4500	1440	3375	4500	3375	3600

Moment of inertia I_x and I_y values in Table 3 have been calculated based on the relationship between I and Δ_{Max} (Table 2) for simply supported beams in classical theory of mechanics. Torsion constant J of CWBs will be equal to the values of WBs listed in Hot Rolled and Structural Steel Products property tables for welded beams (2020), since the flange geometries of CWBs remain the same as the parent WBs. Warping constant is calculated by the formula $I_w = \frac{I_y * {h_d}^2}{4}$ stated in Section 2 of AISC Design Guide 9 (1997), where h_d is the distance between the centroids of two flanges.

Table 3. Essential cross sectional properties of CWBs

	Iy (10^6mm^4)	*J (10^3mm^4)*	*E (MPa)*	*G (MPa)*	*I_w (10^9mm^6)*
700CWB115	70	888	200000	80000	7997
700CWB130	86	1510	200000	80000	9942
700CWB150	98	2690	200000	80000	11496
800CWB122	75.5	921	200000	80000	11366
800CWB146	101	1670	200000	80000	15362
800CWB168	116	2990	200000	80000	17871
900CWB175	116	2060	200000	80000	22458
900CWB218	184	4020	200000	80000	36028
900CWB257	231	6150	200000	80000	45538
1000CWB215	122	2890	200000	80000	29292
1000CWB258	186	4670	200000	80000	45115
1000CWB296	242	7010	200000	80000	59057
1200CWB 249	129	4310	200000	80000	42281
1200CWB278	185	5090	200000	80000	60635
1200CWB313	245	7230	200000	80000	80722

Another set of trial and error FE simulation was performed to find the maximum bending resistance of each CWB after removing the restraints of the top flange, where the corresponding bending capacity M_{non} are expected to smaller than the corresponding fully-restrained CWB, as the beams will experience failure due to twisting of the top flange. Furthermore, the reduction factor values, T_1, shown in Table 4, have been calculated from the relationship between M_{non} and M*.

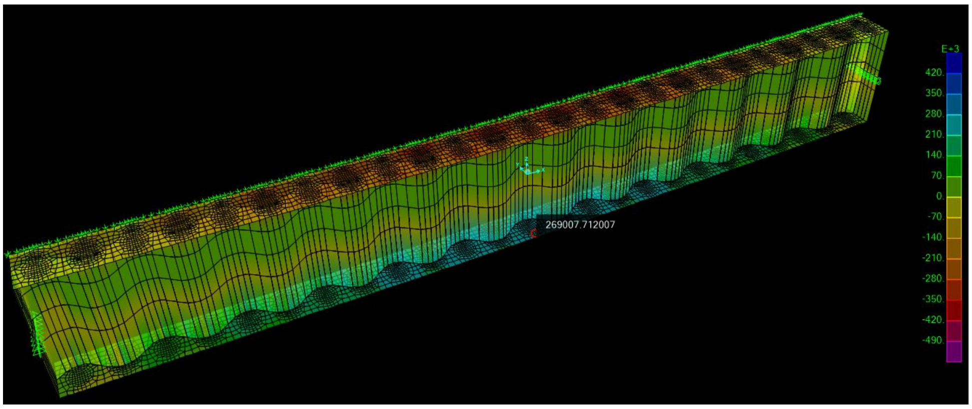

Figure 5. Applying maximum bending moment to the 700CWB115 with fully lateral restrains.

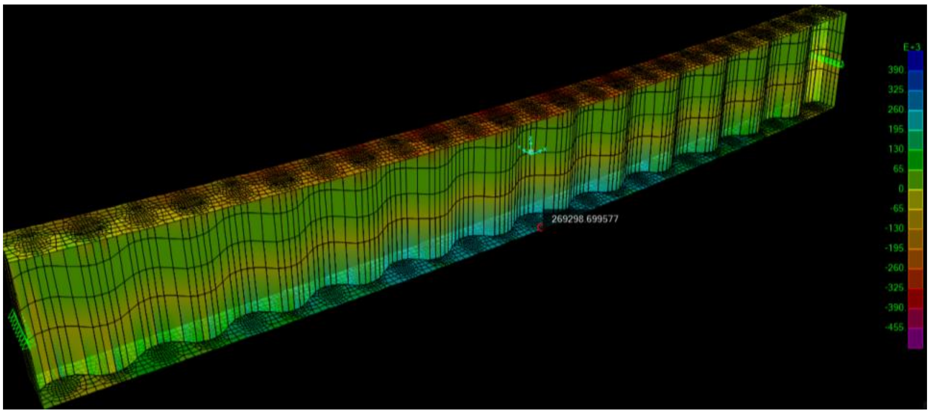

Figure 6. Applying maximum bending moment to the 700CWB without fully lateral restrains.

As illustrated in Figure 5 and Figure 6, both of beams were approaching the flexural strength limit which was 300 MPa*0.9 = 270 MPa. However, it was required about the maximum bending force of 1000 kNm to let the 700CWB115 with fully lateral restrains to approach the strength limit in accordance with AS4100 (1998), while only a bending force of 780 kNm has resulted the 700CWB without fully lateral restrains to reach the yielding stage, where the reduction factor to the real flexural capacity would be 780/1000 = 0.78.

Table 4. Reduction factors from FE models

	M(kNm)*	*M_{non}(kNm)*	*T_1*
700CWB115	1000	780	0.780
700CWB130	1250	980	0.784
700CWB150	1400	1110	0.793
800CWB122	1200	940	0.783
800CWB146	1550	1230	0.794
800CWB168	1740	1400	0.805
900CWB175	1980	1560	0.788
900CWB218	2450	2050	0.837
900CWB257	3000	2540	0.847
1000CWB215	2500	1960	0.784
1000CWB258	3000	2485	0.828
1000CWB296	3520	2980	0.847
1200CWB 249	3000	2340	0.780
1200CWB278	3500	2890	0.826
1200CWB313	4500	3760	0.836

These results from FE investigation show that the effect of the lateral supports on the top flange to resist additional stress from shear-bending interaction is considerably significant, where there is a reduction percentage of between 15-22% in bending capacity as presented in Table 4. However, by comparing to the maximum bending capacity of a fully-restrained 700WB115, the unrestrained 700CWB115 can resist a maximum moment of 780kNm, while the WB can only carry a moment of 850kNm, so it can be considered that the corrugated geometry can increase the stability and provide additional lateral support to the beam.

In general, SAP2000 would present the structure's response to four different buckling modes, including lateral-torsional buckling, flexural-torsional buckling, global buckling and local buckling (Computers and Structures 2020). In this study, the minimum value among those four factors have been selected to compare with the minimum value of 1 to ensure the safety of the web. Table 5 shows that the minimum buckling factors for fully restrained and unrestrained conditions were all greater than 1. The tabulated buckling factor indicate that all the studied corrugated web beams are safe against local buckling.

Table 5. Buckling factor check for CWBs

	Fully restrained	*unrestrained*
700CWB115	6.7957	3.6016
700CWB130	6.5481	4.1274
700CWB150	6.1038	3.8754
800CWB122	5.3619	4.0874
800CWB146	6.0164	4.2514
800CWB168	5.1284	3.0187
900CWB175	6.4498	4.6749
900CWB218	6.2574	4.2541
900CWB257	4.9854	3.2157
1000CWB215	6.3859	5.8691
1000CWB258	7.2584	5.8467
1000CWB296	6.5845	5.4157
1200CWB 249	9.7991	7.6295
1200CWB278	7.5842	6.4571
1200CWB313	8.2415	6.8541

5.2 Numerical Calculations by Using EN1993-1-5

The numerical study has begun with the calculations from the validated method, which has been proven safe by many researchers (Kovesdi et al. 2012; Dunai et al. 2016), to generate the bending moment reduction factor. As mentioned in Section 2, the reduction factors resulted from the shear-bending interaction could appropriately represent the fact that how CWB's strength would be reduced in practical loading conditions. In Equation (5), $L_{EN} = 2 * a_1 + a_4$, so it is equal to half of the corrugation length 400mm, which is 200mm for each CWB, and the amplitude is 57.8mm considering corrugation angle of 30 degree, in which a_3 is equal to 115.6mm. A summary of important parameters for each of the CWBs can be found in Table 6.

Table 6. Mechanical properties of selected CWBs

	L_{EN} (mm)	a_3 (mm)	h_w (mm)	b_f (mm)	t_f (mm)	I_f (mm^4)	f_y (MPa)
700CWB115	200	115.6	660	250	16	20.83	300
700CWB130	200	115.6	660	250	20	26.04	300
700CWB150	200	115.6	660	250	25	32.55	280
800CWB122	200	115.6	760	250	16	20.83	300
800CWB146	200	115.6	760	275	20	34.66	300
800CWB168	200	115.6	760	275	25	43.33	280
900CWB175	200	115.6	860	300	20	45.00	300
900CWB218	200	115.6	860	350	25	89.32	280
900CWB257	200	115.6	860	400	28	149.33	280
1000CWB215	200	115.6	960	300	20	45.00	300
1000CWB258	200	115.6	960	350	25	89.32	280
1000CWB296	200	115.6	960	400	28	149.33	280
1200CWB 249	200	115.6	1120	275	25	43.33	280
1200CWB278	200	115.6	1120	350	25	89.32	280
1200CWB313	200	115.6	1120	400	28	149.33	280

Hence, the reduction factor T_2 stated in EN1993-1-5 (2006) can be computed using Equation (3) to (5). The results are summarised in Table 7. It can be seen from Table 4 and Table 7 that the reduction factors from FE models are slightly smaller than values from the equations. To be on the conservative side, the FE models have given a good approximation to estimate the moment reduction factors taking into account shear-moment interaction. However, the FE simulation models slightly underestimate the reduction factors, which makes the outcomes slightly more conservative.

Table 7. Reduction factors from equations in EN1993-1-5 (2006)

	M_T *(kNm)*	σ_T *(MPa)*	T_2
700CWB115	14.01	84.07	0.788
700CWB130	17.52	84.07	0.788
700CWB150	19.62	75.33	0.800
800CWB122	14.60	87.61	0.784
800CWB146	18.86	74.82	0.800
800CWB168	21.17	67.19	0.811
900CWB175	21.29	70.97	0.805
900CWB218	26.35	51.62	0.834
900CWB257	32.26	43.21	0.848
1000CWB215	24.08	80.28	0.793
1000CWB258	28.90	56.62	0.826
1000CWB296	33.91	45.41	0.844
1200CWB 249	24.77	78.61	0.795
1200CWB278	28.90	56.62	0.826
1200CWB313	37.16	49.76	0.837

5.3 Numerical Calculations Using AS4100

The main focus of this section is to find the reduction factors T_3 from the initial relationships in AS4100 (1998) by using the cross sectional properties of CWBs in Table 3. According to AS4100 (1998), T_3 is a combination of α_m and α_s, and the factor α_m can be assumed to be 1, since the calculated value for α_m is equal to 1.1 from Equation (6). The factor α_s, being the objective of this study, can be calculated using Equation (7) and (8), where the design moment is the state of a loaded beam for each CWB when stress levels are closed to 0.9× f_y for the bending stress or 0.6× f_y for the shear stress. M_o is the reference buckling moment and has been computed using cross sectional properties of each CWB.

Table 8. Reduction factors from equations in AS4100 (1998)

	M_s *(kNm)*	M_o *(kNm)*	T_3
700CWB115	1000	1970.41	0.778
700CWB130	1250	2479.99	0.780
700CWB150	1400	2947.65	0.793
800CWB122	1200	2406.04	0.782
800CWB146	1550	3276.92	0.793
800CWB168	1740	3887.69	0.805
900CWB175	1980	4213.07	0.795
900CWB218	2450	6782.33	0.845
900CWB257	3000	8634.42	0.851
1000CWB215	2500	4950.34	0.779
1000CWB258	3000	7602.67	0.829
1000CWB296	3520	9990.63	0.849
1200CWB249	3000	6124.90	0.786
1200CWB278	3500	8710.89	0.826
1200CWB313	4500	11596.59	0.832

All reduction factors, determined from three different methods, have been summarised in Figure 7 and Table 8 for comparison. Figure 5 clearly indicates that T_2 factors are the highest values for most CWBs. There are 0-2.4% differences between T_1 factors and T_2 factors, while there are 0-1.7% differences between T_2 factors and T_3 factors. The mentioned differences appear to be reasonable and acceptable. Considering the implementation of AS4100(1998), the results from FE models agree well with the results of numerical calculations. Therefore, it has become apparent that the highly structured equations in AS4100 (1998) can provide conservative values with acceptable accuracy.

This study has analysed three different sizes of CWBs in each beam grade listed in the Hot Rolled and Structural Steel Products property tables (2020) to try to verify the capability of the design equations. By comparing three different factors, the major difference is that the T_2 factors of 900CWB grade are less than other two factors, which T_2 factors are the highest values in other four grades. However, all differences are less than 2.5%, which indicates good estimations of the post-buckling strength of each CWB to enable the practicality of the design equations to be applied in the real-world applications. Overall, the equations from EN 1993-1-5 (2006) and AS4100 (1998) could safely predict the post-buckling strength of CWBs redesigning from the Hot Rolled and Structural Steel Products property tables (2020).

In the recent developments of the structural design, achieving more sustainable design has become one of the primary purposes. The better performance, including less usage of materials, better stability and less deflection, strengthen the opportunities of CWBs to be used in practical applications. Despite the slight differences of the reduction factors, it seems safe to conclude that the method presented for determining nominal bending moment capacity in Section 5 of AS4100 (1998) is a safe and accurate method for determining nominal bending capacity of welded steel I-girders with corrugated webs. The validation of the numerical equations from the AS4100 (1998) proved the capability of the steel design standard to estimate the real bending strength of CWBs affected by shear-bending interaction. Eventually, this can create more confidence in Australian practicing engineer's community to use CWBs as the main structural elements and design them confidently using AS4100 (1998).

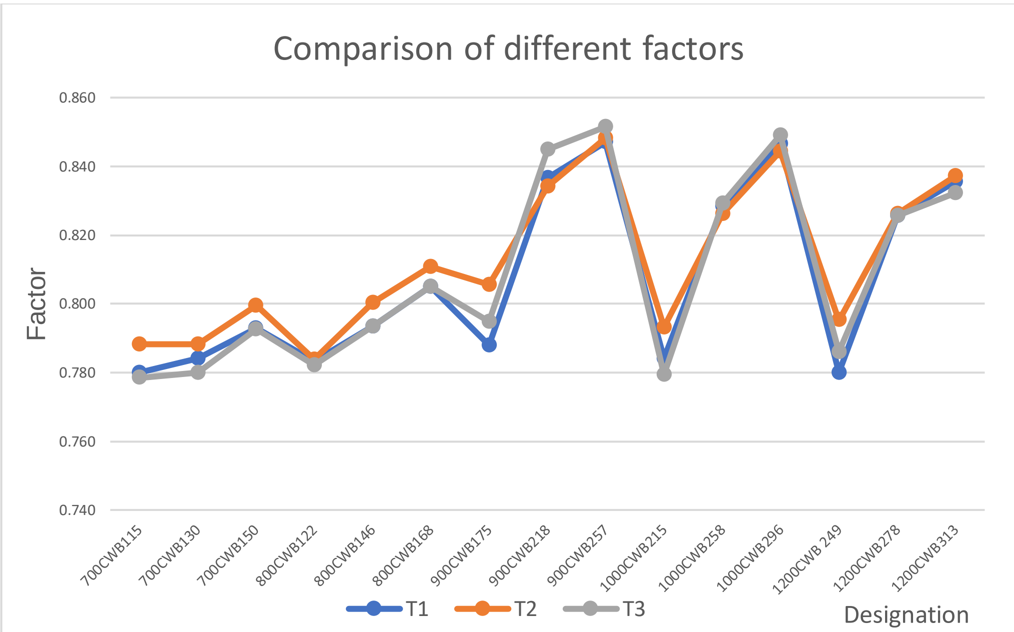

Figure 7. Comparison of different reduction factors

6. Conclusions

In this study, numerical investigations using two different design standards and FE simulations have been carried out to investigate the moment capacity reduction factors for steel I girders with corrugated-web profile affected by shear-moment interaction. Theory of Ultimate Limit State design has been utilised in accordance with AS4100 (1998) in this parametric study along with considering geometric and material non-linearity in the numerical analyses with SAP2000. Comparing the values of this numerical investigation, it has become apparent that the design equations in Section 5 of AS4100 (1998) can adequately estimate the post-buckling strength of corrugated welded beams (CWBs). In particular, the differences in the obtained results from the two studied standards are all less than 2.5%, and some estimated values of reduction factors are even nearly the same. This reasonable variances in estimating the post-buckling strength can not only prove the applicability of the equations in AS4100 (1998) but also promotes better opportunities for CWBs to be utilised in real-world designs. This can create more confidence in Australian practicing engineer's community to use CWBs as the main structural elements and design them confidently using AS4100 (1998). By using AS4100 (1998), engineers and designers in Australian communities can simply use the equations to estimate the post-buckling strength of WBs, while similar equations have not yet been published for CWBs in Australia.

References

Abbas H.H. 2003, 'Analysis and Design of Corrugated Web I-Girders for Bridges Using High-Performance Steel', *PhD dissertation*, Dept. of Civil and Environmental Engineering, Lehigh University.

Abbas H.H., Sause R., Driver R.G. & Asce M. 2006, 'Behavior of Corrugated Web I-Girders under In-Plane Loads', *Journal of Engineering Mechanics*, Vol. 132, No. 8, pp. 806-814.

Aggarwal K., Papangelis J. & Wu S. 2018, 'Finite Element Analysis of Local Shear Buckling in Corrugated Web Beams', Engineering Structures, vol. 162, pp. 37-50.

Alandkar P.M. & Limaye A.A. 2013, 'Strength of Welded Plate Girder with Corrugated Web Plate', *Journal of Engineering Research and Applications*, Vol. 3, No. 5, pp. 1925-1930.

AS/NZS 1170.1 (2002) *Australian/New Zealand Standard and supplement*, *Structural Design Actions – Part 1: Permanent, Imposed and Other Actions*, Standard Australia, Sydney.

AS4100 (1998) *Steel structures*, Standard Australia, Sydney.

Ashrawi M.A., Sunitha C.M. & Smitha K.K. 2016, 'Load Carrying Capacity of Corrugated Web Beams', *International Research Journal of Engineering and Technology*, Vol. 03, No. 09, pp.135-138.

AISD (1997) Design Guide 9: Torsional Analysis of Structural Steel Members, Standard America, Chicago.

Baraket S., Leblouba M. & Al-Saadon Z. 2018, 'Shear Behaviour of Corrugated Web Panels and Sensitivity Analysis', *Journal of Constructional Steel Research*, vol. 151, pp. 94-107.

Calenzani, A.F.G., Fakury, R.H., Fernando Paula, F.A., Rodrigues, F.C., Queiroz, G. & Pimenta, R.J. 2012 'Rotational stiffness of continuous composite beams with sinusoidal-web profiles for lateral-torsional buckling', *Journal of Constructional Steel Research*, vol. 79, pp. 22-33.

Computers and Structures 2020, CSI Analysis Reference Manual for SAP2000, Berkeley, California. <https://docs.csiamerica.com/manuals/sap2000/CSiRefer.pdf#page=1>>.

Divaha R. & Joanna P.S. 2016, 'Investigation on the Behaviour of Encased Cold-formed Steel Beams with Trapezoidally Corrugated Web', *International Journal of Chemistry Science*, Vol. 14, pp. 10-16.

Dubina D., Ungureanu V. & Gilia L. 2015, 'Experimental Investigations of Cold-Formed Steel Beams of Corrugated Web and Built-up Section for Flanges', *Thin-Walled Structures*, Vol. 90, pp. 159-170.

Dunai L., Jáger B. & Kövesdi B. 2016, 'Bending and Shear Interaction Behaviour of Girders with Trapezoidally Corrugated Webs', *Journal of Constructional Steel Research*, vol. 121, pp. 383-97.

Elchalakani M., Elkawas A. A. & Hassanein M.F. 2018, 'Lateral-torsional Buckling Strength and Behaviour of High-strength Steel Corrugated Web Girders for Bridge Construction', *Thin-walled Structures*, vol. 122, pp. 112-123.

EN 1993-1-5 (2006) Design of Steel Structures Part 1-5: Plated Structural Elements, Eurocode 3, Brussels.

Oliveira, J.P.S., Calenzani, A.F.G, Fakury, R.H., Ferreira, W. 2016 'Elastic critical moment of continuous composite beams with a sinusoidal-web steel profile for lateral-torsional buckling', *Engineering Structures*, vol. 113, pp. 121-132.

He J., Wang S., Liu Y. Zhan L. & Li C.X. 2017, 'Mechanical Behaviour of a Partially Encased Composite Girder with Corrugated Steel Web Interaction of Shear and Bending', *Engineering*, vol. 3, pp. 806-816.

Hot Rolled and Structural Steel Products, Welded Beams, viewed May 2020, https://www.libertygfg.com/media/165356/seventh-edition-hot-rolled-and-structural-steel-productsseventh-edition-hot-rolled-and-structural-steel-products.pdf

Huang L., Hikosaka H. & Komine K. 2004, 'Simulation of Accordion Effect in Corrugated Steel Web with Concrete Flanges', *Computers and Structures*, Vol. 82, pp. 2061-2069.

Joanna P. S. & Divahar R. 2018, 'Numerical Simulation and Experimental Investigation on Static Behaviour of Cold Formed Steel Beam with Trapezoidally Corrugated Web by Varying Depth-thickness Ratio', *Asian Journal of Civil Engineering*, vol. 19, pp. 121-137.

Li X.L., Wang Z. Y. & Zhang T. 2019, 'Experimental and Numerical Study of Residual Stress Distribution of Corrugated Web I-beams', *Journal of Constructional Steel Research*, vol. 76, pp. 112-120.

Lin X.Q., Far H. & Saleh A. 2018, "Structural Behaviour and Mechanical Properties of Welded Steel I-Girders with Corrugated Webs", *International Journal of Steel Structures*, Vol. 19, pp 1342-1352.

Lukin A &. Shlyakhin D. 2016, 'A Flexible Beam with Corrugated Web and Its Performance under Bending: An Experimental Study', *MATEC Web of Conferences*, Vol. 86, pp. 44-53.

Maali M. 2019, 'Experimental and Numerical Prediction of Torsional Behaviour of Steel Beam with Sinusoidal Web', *Iranian Journal of Science and Technology*, viewed at 20th March 2020, https://doi.org/10.1007/s40996-019-00304-9

Martins, A. G., Fakury, R.H, Pimenta, R. J., Queiroz, G. & Rodrigues, F.C. 2012 'Moment resistance of composite steel and concrete connection in sinusoidal-web girders', *Journal of Constructional Steel Research*, vol. 76, pp. 112-120.

Walsh, P., Saleh. A. and Far, H. 2018 'Evaluation of Structural Systems in Slender High-rise Buildings', *Australian Journal of Structural Engineering*, vol. 19, no. 2, pp. 105-117.

Yazeed E. S. 2007, 'Design Aspects of Steel I-Girders with Corrugated Steel Webs', *Electronic Journal of Structural Engineering*, Vol. 7, pp. 27-40.

Zhou M., Shang X.N., Hassanein M. F. & Zhou L.Y. 2019, 'The Differences in the Mechanical Performance of Prismatic and Non-prismatic Beams with Corrugated Steel Webs: A Comparative Research', *Thin-Walled Structures*, vol. 141, pp. 40-410.